Article

JOURNAL OF COMPOSITE MATERIALS

Journal of Composite Materials
2016, Vol. 50(9) 1247–1260

DOI: 10.1177/0021998315590264
jcm.sagepub.com
SAGE

Microplane triad model for simple and accurate prediction of orthotropic elastic constants of woven fabric composites

Kedar Kirane[1], Marco Salviato[2] and Zdeněk P Bažant[3]

Abstract

An accurate prediction of the orthotropic elastic constants of woven composites from the constituent properties can be achieved if the representative unit cell is subdivided into a large number of finite elements. But this would be prohibitive for microplane analysis of structures consisting of many representative unit cells when material damage alters the elastic constants in each time step in every element. This study shows that predictions almost as accurate and sufficient for practical purposes can be achieved in a much simpler and more efficient manner by adapting to woven composites the well-established microplane model, in a partly similar way as recently shown for braided composites. The undulating fill and warp yarns are subdivided into segments of different inclinations and, in the center of each segment, one microplane is placed normal to the yarn. As a new idea, a microplane triad is formed by adding two orthogonal microplanes parallel to the yarn, one of which is normal to the plane of the laminate. The benefit of the microplane approach is that it is easily extendable to damage and fracture. The model is shown to give realistic predictions of the full range of the orthotropic elastic constants for plain, twill, and satin weaves and is extendable to hybrid weaves and braids.

Keywords

Fabrics/textiles, mechanical properties, microstructures, computational modeling, laminates, deformation, stress analysis

Introduction

Owing to their light weight and high specific strength, stiffness and toughness, woven fiber composites have become attractive alternatives to metals in aerospace, automotive, marine, and defense applications. To optimize the engineering design of these components, physics-based constitutive modeling of the material on the sub-scale is essential. The input of most conventional continuum models uses the elastic properties of the individual lamina semi-empirically. However, a change in the weave type necessitates repeat testing of all the mechanical properties of the laminate, despite having the same constituents. This repetition can be avoided by setting up a predictive model whose lamina properties on the meso-scale could be calibrated by tests for one weave type and then used in a similar way for another weave type.

The literature abounds with analytical and numerical formulations that achieve this goal with varying degrees of success (see a comprehensive review in literature[1–3]). The effect of waviness and buckling of compressed yarn embedded in a polymer was introduced in 1968[4] in an analytical model that gave very realistic predictions of axial stiffness (for a summary see Sec. 11.9 in Bažant and Cedolin[5]). Later, important analytical models were proposed in the 1980s by Ishikawa and Chou.[6,7] Ishikawa and Chou[6] proposed a "mosaic model" which idealizes the woven fabric as an assembly of cross-ply laminates and provides upper and lower bounds for the elastic properties of laminate. Further, they developed the "fiber undulation model"[6] which, like,[4] accounts for the knee behavior of plain weave fabric composites and the yarn continuity, but again only in the loading direction. Their third model, the "bridging model", also accounts for the load transfer among the interlaced regions in satin composites.[7]

[1]Department of Mechanical Engineering, Northwestern University, IL, USA
[2]Department of Civil and Environmental Engineering, Northwestern University, IL, USA
[3]Department of Civil and Environmental, Material Science and Mechanical Engineering, Northwestern University, IL, USA

Corresponding author:
Zdeněk P Bažant, Northwestern University, 2145 Sheridan Rd, #A135 Evanston, IL 60208, USA.
Email: z-bazant@northwestern.edu

Again, this model considers the undulation in the loading direction, but not the transverse direction. Besides, the effects of the cross section geometry of the yarn are not considered.

A two-dimensional (2D) model that accounts for the yarn cross section geometry and the gaps between yarns was proposed by Naik and Ganesh[8] but the out-of-plane stresses were not captured. Another similar example was the generalized 2D model of Hahn and Pandey,[9] which predicted not only the effective elastic moduli but also the linear thermal expansion coefficient. There also exist several models based on the so-called Classical Laminate Theory (CLT). An example is the model developed by Scida et al.[10] called MESOTEX, intended for hybrid and non-hybrid woven composites.

The most accurate predictions of the effective lamina properties have been obtained by large-scale three-dimensional (3D) finite element simulations of the representative unit cell (RUC); see e.g.[11–18] This involves a detailed meshing of the RUC microstructure, including the undulating yarns, with explicit resolution of the contact between them. Although the calculated effective lamina properties are very accurate, the programming is not simple and requires tedious pre-processing, especially for complex weaves. More importantly, one has to cope with a very high number of degrees of freedom per RUC, which is a prohibitive computational burden in systems of many RUCs when damage alters the elastic constants of each RUC at each load step and prevents repetitive use of the same elastic constants. The advantages of the foregoing approaches could be combined in a simple, semi-analytical framework that can (1) predict all the orthotropic elastic constants in an efficient manner and (2) merge seamlessly with a material point level continuum damage model. Such a framework is developed here, based on the microplane theory.

The microplane theory was originally developed to describe the softening damage of heterogeneous, but statistically isotropic materials such as concrete and rocks.[19–21] The basic idea of the microplane model is to express the constitutive law in terms of the stress and strain vectors acting on a generic plane of any orientation within the material meso-structure, called the microplane. The microplane strain vectors are the projections of the macroscropic strain tensor, whereas the macroscopic stress tensor is obtained from the microplane stress vectors via the principle of virtual work. The use of vectors in a constitutive model was the idea of Taylor.[22] It helps physical insight and makes the constitutive law conceptually clear. Taylor's idea has been used extensively for plasticity of polycrystalline metals, in which the stress, rather than the strain, tensor is projected onto the microplanes and the plastic strain vectors are then superposed to give the plastic strain tensor (for a review, cf. Brocca and Bažant[23]). The static constraint, though, is limited to non-softening inelastic strain. For softening, it would make the material model unstable[19] and so a kinematic constraint must be employed.

Several approaches to apply the microplane concept to orthotropic materials have been explored.[24–26] However, the role played by the meso-scale constituents (e.g. fibers and matrix) in determining the overall elastic behavior was not clarified in these studies. This was later attempted in Caner et al.[27] where the microplane theory was applied to orthotropic 2D triaxially braided composites. They considered microplanes only with a specific orientation, a concept equivalent to assigning zero stiffness to microplanes of other orientations and thus automatically introducing orthotropy. In addition to the previously mentioned benefit of a vectorial formulation, an added advantage became evident in Caner et al.[27] It was realized that the same microplanes that describe the damaging behavior can also be used to predict the elastic constants of the lamina from the properties of the individual constituents and the details of the meso-structure geometry. The preferentially oriented microplanes allow physically intuitive inclusion of the effects of yarn undulations and aspect ratio on the stiffness and load transfer mechanisms.

However, this advantage was not fully realized in Caner et al.,[27] where only the axial elastic properties of the laminate were predicted well. Presented here is microplane theory improved by a new concept—the microplane triads. It can predict realistically all the macro-scale orthotropic elastic constants of woven composites, including the shear stiffness and Poisson effects. The model is shown to have sufficient generality, allowing attractive extensions to more complex architectures such as hybrid woven composites, and two- or three-dimensionally braided composites. Similar to Caner et al.[27] this model also is computationally efficient and readily extendable to a point-wise continuum damage constitutive model, suitable for analyzing damage and fracture of large composite structures. Here, however, the goal is to showcase the versatility of the model in predicting the elastic properties of various woven composites. Application of this framework to a damage model is relegated to a follow-up article.

Microplane theory for woven textile composites

Representative unit cell

A woven composite consists on the meso-scale of a polymer resin matrix reinforced by two sets of yarns interlaced perpendicularly to one another. The two

sets are referred to as the fill (or weft) yarns and the warp yarns. The yarns themselves consist of fiber bundles with matrix between the fibers. Different types of fibers (such as carbon, E-glass, aramid and polyester fibers) as well as various types of weave architectures are commonly employed, depending on the specific application. The weave type is governed by the number of yarns skipped per weave. For example, in a plain weave, the fill yarn skips over every other warp yarn and vice versa, while for the twill weave, it skips over every two warp yarns.[28,29]

The microplane model characterizes at one continuum point the average behavior of one RUC, defined as the smallest geometric unit that gets periodically repeated within the woven composite. For one RUC, we introduce a local co-ordinate system such that coordinates 1 and 2 represent the fill and warp yarn directions, respectively. Then, the local direction 3 is the out-of-plane normal, as shown in Figure 1(a) for a twill 2×2 woven composite.

Each RUC is imagined to consist of three plates, namely: (1) the fill yarn plate; (2) the warp yarn plate and (3) the pure matrix (or polymer) plate (Figure1(b)). These plates are assumed to act in parallel coupling.[16,27] The elastic stiffness tensor of the RUC is then expressed as

$$\mathbf{K}^{RUC} = \frac{V_y}{2}\mathbf{K}^{FY} + \frac{V_y}{2}\mathbf{K}^{WY} + (1 - V_y)\mathbf{K}^{M} \tag{1}$$

where $\mathbf{K}^{RUC}$, $\mathbf{K}^{FY}$, $\mathbf{K}^{WY}$ and $\mathbf{K}^{M}$ represent the fourth-order stiffness tensors of the RUC, fill yarn plate, warp yarn plate, and pure matrix plate, respectively, and V_y is the volume fraction of the yarn (or the tow) within one RUC. It should be noted that this is the volume fraction not of the pure fiber (V_f), but of the yarn within the RUC. The yarn itself consists of some matrix material (or polymer) that lies between the individual fiber strands. The yarn volume fraction V_y within one RUC is expressed as

$$V_y = \frac{\text{volume fraction of fiber within one RUC}}{\text{volume fraction of fiber within one yarn}} = \frac{V_f}{V_f^Y} \tag{2}$$

Equation (1) indicates how to predict the elastic stiffness tensor of one RUC from the stiffness tensors of its constituents at the lower scale. How to derive each of these constituent stiffness tensors is described next.

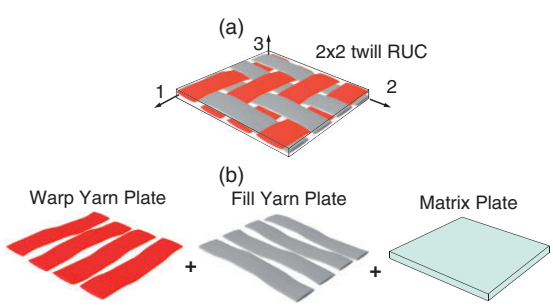

Figure 1. Schematic representation of (a) the RUC of a 2×2 twill composite and its local coordinate system; (b) decomposition of the RUC into matrix, fill, and warp yarn plates assumed to be in parallel coupling.
RUC: representative unit cell.

Stiffness tensor of the matrix plate

Since the matrix is isotropic, its fourth-order stiffness tensor is given by

$$K^M_{ijkl} = \frac{E^m}{3(1-2\nu^m)}\delta_{ij}\delta_{kl} + \frac{E^m}{2(1+\nu^m)}\left(\delta_{ik}\delta_{jl} + \delta_{il}\delta_{jk} - \frac{2}{3}\delta_{ij}\delta_{kl}\right) \tag{3}$$

Here subscripts i, j, k, l run from 1 to 3 and δ_{ij} is Kronecker delta or the second-order identity tensor, such that $\delta_{ij} = 1$ when $i = j$ and $\delta_{ij} = 0$ when $i \neq j$. E^m and ν^m denote the Young's modulus and Poisson ratio of the matrix.

Stiffness tensor of the yarn plates

The stiffness tensor of the yarn plates (fill and warp) is now derived by applying the microplane theory. To describe the yarn stiffness, the portion of the undulating yarn within the RUC is subdivided into several segments of different inclinations. Each segment is represented by a triad of orthogonal microplanes, oriented such that one of the microplane normals, **n**, be always tangential to the yarn curve at the segment center, and one other microplane have a normal vector **m** parallel to the yarn plate.

Then, the stiffness tensors of the yarn plates $\mathbf{K}^{FY}$ and $\mathbf{K}^{WY}$ are obtained by imposing strain energy density equivalence. It is stipulated that the strain energy density at yarn plate level T^{YP} be equal to the volume averaged strain energy density at microplane level T^{μ}. Then

$$T^{YP} = \frac{1}{AL}\int_V T^{\mu}\mathrm{d}V = \frac{1}{L}\int_L T^{\mu}\mathrm{d}L \tag{4}$$

where A is the yarn plate cross section area, L is the curvilinear length of the yarn, V is the yarn plate volume $= AL$ and $dV = AdL$.

The foregoing integral is unbiased and exact if there is an infinite number of microplane triads along the yarn. Here we propose a discretized approximate equivalent

this integral. This is achieved by discretizing the portion of the undulating yarn within the RUC into several segments, as shown in Figure 2(a). For the identified RUC of woven composites, at least six yarn segments are required to discretize the undulating yarn path.

One microplane triad is introduced for each yarn segment. It is oriented such that the normal **n** of one of the three microplanes be parallel to the yarn curve at the center of the segment. From the angle of that normal with respect to the yarn plate, denoted as α (Figure 2(a)), the direction cosines of the normals of all the microplanes in the triad follow. For each triad, vectors **m** and **l** are normal to the local yarn direction. The vectors **n**, **m,** and **l** form a right-handed triad of vectors.

Angle α is related to the aspect ratio of the elliptical yarn cross section and is given by $\alpha = \tan^{-1}[b_y/(a_y + g_y)]$ where a_y is the major axis, b_y is the minor axis (equal to the yarn thickness), and g_y is the average gap between the yarns. Microplane triads are introduced in both the fill and warp directions. Due to the assumed symmetry, the α values for both the fill and warp yarns are the same. Then, the microplanes for the warp yarn are nothing but the fill yarn microplanes rotated by 90° about the RUC coordinate vector 3. Note that a different undulation angle for the fill and warp yarns could easily be used when dealing with another composite.

Integral (4) can be discretely approximated as a weighted average of the strain energy density of all six microplane triads

$$T^{YP} = \sum_{\mu=1}^{6} w^{\mu} T^{\mu} \tag{5}$$

Here μ is the number of the microplane triads, and w^{μ} is its weight, given by $w^{\mu} \approx L^{\mu}/L$, where L^{μ} is the length of the yarn segment corresponding to the microplane triad μ. Thus, the microplane triad stiffness is weighted in proportion to the fraction of yarn length occupied by that orientation. E.g., for a plain weave the weights for each microplane triad would be mutually equal and have the value of 1/6, but for a satin weave they would be unequal. The weights are normalized by the partition of unity, so $\sum_{\mu=1}^{6} w^{\mu} = 1$. Note that, as opposed to the standard iso-strain assumption, the present microplane model with the aforementioned weighted sum allows a different projected strain on the various microplanes, to account for the effect of the undulating yarn.

Once the total strain energy density is computed, the stiffness tensor of the yarn plate is defined as

$$K^{YP}_{ijkl} = \frac{\partial^2 T^{YP}}{\partial \epsilon_{ij} \partial \epsilon_{kl}} \tag{6}$$

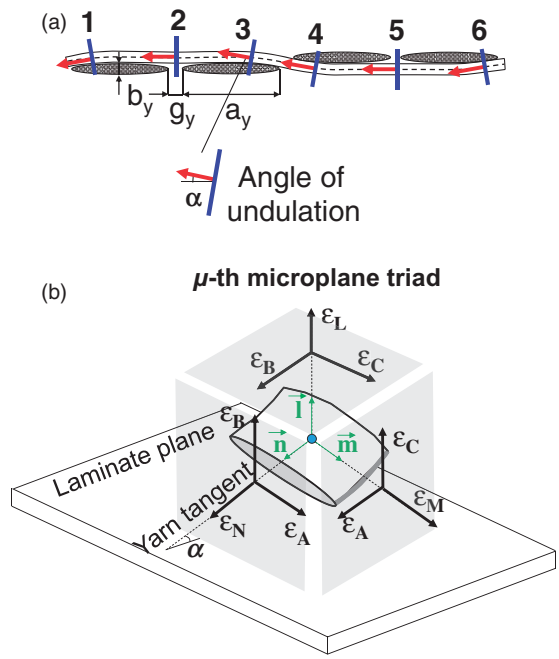

Figure 2. Example of discretization of the yarn into microplanes for a twill 2 × 2; (b) projection of the strain tensor into the μth microplane triad.

which provides the following final equation

$$K^{YP}_{ijkl} = \frac{\partial^2}{\partial \epsilon_{ij} \partial \epsilon_{kl}} \left(\sum_{\mu=1}^{6} w^{\mu} T^{\mu} \right) = \sum_{\mu=1}^{6} w^{\mu} \frac{\partial^2 T^{\mu}}{\partial \epsilon_{ij} \partial \epsilon_{kl}} = \sum_{\mu=1}^{6} w^{\mu} K^{\mu}_{ijkl} \tag{7}$$

where K^{μ}_{ijkl} represents the stiffness tensor at microplane level, and is derived next. This approach is a conceptual parallel to the principle of virtual work, used in the conventional microplane model for statistically isotropic particulate composites (e.g. concrete) to relate the macro and microplane stresses. Since here the focus is on the elastic properties only, it suffices to use the strain energy equivalence. Both approaches are identical, except that, in the end, the stiffness tensors in equation (7) are replaced by the stress tensors corresponding to the strain tensor.

It should also be noted that the stiffness tensor calculated in equation (7) is the result of a homogenization over all the microplanes describing the yarn, which is characterized by different projected strains. While this approach does not aim at being as accurate as a full 3D-FE simulation, it appears to be an effective way to describe the effects of the mesostructure, with the intriguing possibility to extend the model to damage. In fact, the slightly lower accuracy is largely compensated by computational efficiency, which allows the simultaneous modeling of many RUCs required for

damage and fracture analysis of large composite structures.

Stiffness tensor at microplane level

The stiffness tensor for one microplane triad is derived from the elastic properties of the constituents, i.e. the fibers and matrix. Each microplane triad represents a segment of the yarn which is considered as a uni-directional, transversely isotropic, composite consisting of pure fibers and inter-fiber matrix. The macroscopic strain tensor ϵ_{ij} is projected on each microplane of each triad (Figure 2(b)). The normal microplane strain ϵ_N is given by

$$\epsilon_N = \epsilon_{ij} n_i n_j \tag{8}$$

and the transverse normal strains in the triad are given by

$$\epsilon_M = \epsilon_{ij} m_i m_j \qquad \epsilon_L = \epsilon_{ij} l_i l_j \tag{9}$$

Furthermore, ϵ_A, ϵ_B and ϵ_C are the shear strain vectors that are given by

$$\begin{aligned} \epsilon_A &= \frac{1}{2}\epsilon_{ij}(n_i m_j + m_i n_j) \quad \epsilon_B = \frac{1}{2}\epsilon_{ij}(n_i l_j + l_i n_j) \\ \epsilon_C &= \frac{1}{2}\epsilon_{ij}(m_i l_j + l_i m_j) \end{aligned} \tag{10}$$

These strain vectors are now used to derive the full fourth-order stiffness tensor for the microplane triad. While in previous formulations of the microplane model, ϵ_M and ϵ_L denoted the shear strain vectors, here they denote the transverse normal strain vectors. The shear strain vectors are denoted by ϵ_A, ϵ_B, and ϵ_C.

This change in notation is necessary because of using microplane triads instead of individual microplanes. Herein lies the essential difference of the present microplane model from the conventional microplane models for statistically isotropic materials. In the conventional models for statistically isotropic materials, the orientations of microplane normals sample the optimal Gaussian integration points for the evaluation of an integral over all spatial directions (i.e. over the surface of a hemisphere). Each of these microplanes is characterized by the normal strain and two shear strains. Refining the Gaussian integration scheme converges to the integral, which guarantees tensorial invariance. The normal and shear moduli on the microplanes control the values of the macroscopic shear moduli and Poisson ratio.

For an orthotropic material the invariance restrictions are different and more complex. The present approach with microplane triads representing the well-defined microstructure avoids dealing with these restrictions and produces an orthotropic material stiffness tensor directly. It is important that each microplane triad is characterized by three normal strains, one for each microplane in the triad, and three shear strain components (note that each shear strain is common to two microplanes in the triad). Note that in the plane normal to the yarn segment, the response of the yarn segment is isotropic.

A properly representative choice of microplanes is, of course, important. This is exemplified by comparison with the preceding model[27] that featured the microplanes normal to yarn segments but missed the microplanes parallel to the yarn. That model, applied to a braided composite, could not capture the Poisson and shear effects accurately.

Another difference from the previous formulation in Caner et al.[27] is the use of the strain energy approach to derive the stiffness tensor for each microplane triad. Although the equilibrium conditions obtained by derivatives of strain energy are equivalent to those expressed by the principle of virtual work in previous microplane models, the present energy approach is convenient for ensuring the inclusion of all the deformation modes, including the volumetric and deviatoric ones, and for automatically capturing the Poisson and shear effects.

Accordingly, the strain energy density for one microplane triad T^μ is written as[30]

$$\begin{aligned} T^\mu = {} & A_1\epsilon_N^2 + A_2\epsilon_M^2 + A_3\epsilon_L^2 + \frac{A_4}{2}(\epsilon_N\epsilon_M + \epsilon_M\epsilon_N) \\ & + \frac{A_5}{2}(\epsilon_N\epsilon_L + \epsilon_L\epsilon_N) + \frac{A_6}{2}(\epsilon_M\epsilon_L + \epsilon_L\epsilon_M) \\ & + A_7\epsilon_A^2 + A_8\epsilon_B^2 + A_9\epsilon_C^2 \end{aligned} \tag{11}$$

where $A_1, A_2 \ldots A_9$ are functions of the elastic constants of the unidirectional composite yarn, and will be described later.

Substituting equation (8) in the first term of the foregoing expression, we get

$$T_1 = A_1\epsilon_N^2 = A_1(\epsilon_{ij}n_i n_j)^2 \;=\; A_1(\epsilon_{ij}n_i n_j)(\epsilon_{kl}n_k n_l) \tag{12}$$

(index repetition implies summation). Similarly, the second and third term become

$$T_2 = A_2(\epsilon_{ij}m_i m_j)(\epsilon_{kl}m_k m_l)\,; \quad T_3 = A_3(\epsilon_{ij}l_i l_j)(\epsilon_{kl}l_k l_l) \tag{13}$$

Terms 4 to 6 involve cross terms, and become

$$\begin{aligned} T_4 &= \frac{A_4}{2}\left[(\epsilon_{ij}n_i n_j)(\epsilon_{kl}m_k m_l) + (\epsilon_{ij}m_i m_j)(\epsilon_{kl}n_k n_l)\right] \\ T_5 &= \frac{A_5}{2}\left[(\epsilon_{ij}n_i n_j)(\epsilon_{kl}l_k l_l) + (\epsilon_{ij}l_i l_j)(\epsilon_{kl}n_k n_l)\right] \\ T_6 &= \frac{A_6}{2}\left[(\epsilon_{ij}m_i m_j)(\epsilon_{kl}l_k l_l) + (\epsilon_{ij}l_i l_j)(\epsilon_{kl}m_k m_l)\right] \end{aligned} \tag{14}$$

Likewise, terms 7 to 9 are given by

$$\begin{aligned} T_7 &= A_7(\epsilon_{ij}a_ia_j)(\epsilon_{kl}a_ka_l) \\ T_8 &= A_8(\epsilon_{ij}b_ib_j)(\epsilon_{kl}b_kb_l) \\ T_9 &= A_9(\epsilon_{ij}c_ic_j)(\epsilon_{kl}c_kc_l) \end{aligned} \tag{15}$$

where $a_ia_j = 1/2(n_im_j + m_in_j)$, $b_ib_j = 1/2(n_il_j + l_in_j)$ and $c_ic_j = 1/2(m_il_j + l_im_j)$. Now, substituting the above in equation (11) and taking twice the derivative with respect to the strain tensor, we obtain the expression for the stiffness matrix of one microplane triad as

$$K^{\mu}_{ijkl} = \frac{\partial^2 T^{\mu}}{\partial\epsilon_{ij}\partial\epsilon_{kl}} = K^{N\mu}_{ijkl} + K^{P\mu}_{ijkl} + K^{S\mu}_{ijkl} \tag{16}$$

Here the three right-hand-side terms represent various parts of the stiffness tensor. $K^{N\mu}_{ijkl}$ represents the normal stiffness in the axial and transverse directions, $K^{P\mu}_{ijkl}$ the Poisson effects and $K^{S\mu}_{ijkl}$ the shear stiffness.

Due to the well-defined roles of the microplane strain vectors, the individual contributions of each term in the strain energy density expression to the stiffness tensor can easily be clarified. The first three terms contribute to the normal stiffness $K^{N\mu}_{ijkl}$ in the axial and transverse directions, given by

$$K^{N\mu}_{ijkl} = 2A_1n_in_jn_kn_l + 2A_2m_im_jm_km_l + 2A_3l_il_jl_kl_l \tag{17}$$

Terms 4 to 6 contribute to the Poisson effects, and are written as

$$\begin{aligned} K^{P\mu}_{ijkl} = &\frac{A_4}{2}(n_in_jm_km_l + m_im_jn_kn_l) + \frac{A_5}{2}(n_in_jl_kl_l + l_il_jn_kn_l) \\ &+ \frac{A_6}{2}(m_im_jl_kl_l + l_il_jm_km_l) \end{aligned} \tag{18}$$

Lastly, terms (7) to (9) represent the shear stiffness and are included in K^{S}_{ijkl} as

$$K^{S\mu}_{ijkl} = 2A_7(a_ia_ja_ka_l) + 2A_8(b_ib_jb_kb_l) + 2A_9(c_ic_jc_kc_l) \tag{19}$$

Together, these three terms yield the complete stiffness tensor for one microplane triad. See the appendix for a simple demonstrative example.

Effective elastic properties of the yarn

To explain parameters $A_1, A_2 \ldots A_9$ that populate the microplane triad stiffness tensor, the effective properties of the yarn are calculated first using a meso-mechanics approach. Let the superscript Y denote the yarn properties, m the matrix properties and f the pure fiber properties. In this context, the term "matrix" now implies the matrix in between the pure fibers within one yarn.

Various meso-scale simulations suggest that the matrix between the fibers within a yarn works in transferring the loads in the lateral direction and stiffens the axial response. This may be approximated by considering a parallel coupling of the matrix with pure fibers in the axial direction, but a series coupling in the transverse direction. As will be seen later, the calculated yarn properties are in satisfactory agreement with the values from experiments (it is nevertheless possible that using more advanced rules of mixtures, such as the self-consistent concentric cylinder model[31] could further improve the predictions). Accordingly, we have, for the yarn

$$E^Y_{1'} = V^Y_f E^f_{1'} + (1 - V^Y_f)E^m \tag{20}$$

where $E^Y_{1'}$ is the axial modulus of the yarn, $E^f_{1'}$ is the axial modulus of the fiber, E^m the modulus of the matrix and V^Y_f is the fiber volume fraction within one yarn. For the transverse directions we assume a series coupling. So

$$E^Y_{2'} = E^Y_{3'} = \left(\frac{V^Y_f}{E^f_{2'}} + \frac{1 - V^Y_f}{E^m}\right)^{-1} \tag{21}$$

where $E^Y_{2'} = E^Y_{3'}$ and $E^f_{2'} = E^f_{3'}$ are transverse moduli of the yarn and the fibers, respectively. Here the suffix $1'$ denotes the axial direction of the yarn, while the plane $2' - 3'$ is the cross section of the yarn as shown in Figure 3. The "prime" is introduced to distinguish from the RUC co-ordinate system (where direction 1 is the fill yarn, and direction 2 the warp).

For the in-plane shear response, it is common to assume a self-consistent scheme of coupling[32] which

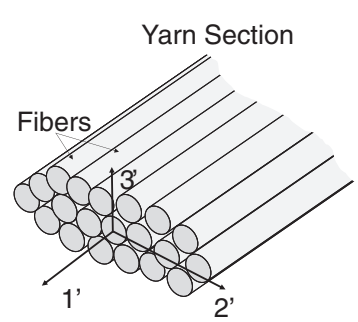

Figure 3. Local coordinate system assigned to each yarn section.

provides better estimates compared to a pure series coupling. Accordingly

$$G^Y_{1'2'} = G^Y_{1'3'} = G^m \frac{(G^f_{1'2'} + G^m) + V^Y_f(G^f_{1'2'} - G^m)}{(G^f_{1'2'} + G^m) - V^Y_f(G^f_{1'2'} - G^m)} \quad (22)$$

For the out-of-plane shear elastic modulus, a series, rather than parallel, coupling is appropriate. So

$$G^Y_{2'3'} = \left(\frac{V^Y_f}{G^f_{2'3'}} + \frac{1 - V^Y_f}{G^m}\right)^{-1} \quad (23)$$

where $G^Y_{1'2'}, G^Y_{1'3'}, G^Y_{2'3'}$ represent the shear moduli of the yarn, $G^f_{1'2'}, G^f_{1'3'}, G^f_{2'3'}$ the shear moduli of the fiber and $G^m = E^m/2(1+\nu^m)$ the shear modulus of the matrix.

For all the Poisson ratios of the yarn, we assume the following relations

$$\begin{aligned} \nu^Y_{1'2'} &= V^Y_f \nu^f_{1'2'} + (1 - V^Y_f)\nu^m; \\ \nu^Y_{1'3'} &= V^Y_f \nu^f_{1'3'} \quad + (1 - V^Y_f)\nu^m; \\ \nu^Y_{2'3'} &= V^Y_f \nu^f_{2'3'} + (1 - V^Y_f)\nu^m \end{aligned} \quad (24)$$

These effective properties are used to obtain the fourth-order elasticity tensor of the yarn. Noting that $1' - 2'$, $1' - 3'$, and $2' - 3'$ are three planes of material symmetry, the elastic tensor of the yarn, denoted as C_{pq} (p, q = 1 to 6), can be written as follows

$$\begin{bmatrix} \sigma_{1'} \\ \sigma_{2'} \\ \sigma_{3'} \\ \tau_{1'2'} \\ \tau_{2'3'} \\ \tau_{1'3'} \end{bmatrix} = \begin{bmatrix} C_{1'1'} & C_{1'2'} & C_{1'3'} & 0 & 0 & 0 \\ C_{1'2'} & C_{2'2'} & C_{2'3'} & 0 & 0 & 0 \\ C_{1'3'} & C_{2'3'} & C_{3'3'} & 0 & 0 & 0 \\ 0 & 0 & 0 & C_{4'4'} & 0 & 0 \\ 0 & 0 & 0 & 0 & C_{5'5'} & 0 \\ 0 & 0 & 0 & 0 & 0 & C_{6'6'} \end{bmatrix} \times \begin{bmatrix} \epsilon_{1'} \\ \epsilon_{2'} \\ \epsilon_{3'} \\ \gamma_{1'2'} \\ \gamma_{2'3'} \\ \gamma_{1'3'} \end{bmatrix} \quad (25)$$

The various C_{pq} are obtained from the effective yarn properties as[32]

$$C^Y_{1'1'} = \frac{1 - \nu^Y_{2'3'}\nu^Y_{3'2'}}{E^Y_{2'}E^Y_{3'}\Delta}; \quad C^Y_{2'2'} = \frac{1 - \nu^Y_{1'3'}\nu^Y_{3'1'}}{E^Y_{1'}E^Y_{3'}\Delta}; \quad C^Y_{3'3'} = \frac{1 - \nu^Y_{1'2'}\nu^Y_{2'1'}}{E^Y_{1'}E^Y_{2'}\Delta} \quad (26)$$

and

$$C^Y_{1'2'} = \frac{\nu^Y_{1'2'} + \nu^Y_{1'3'}\nu^Y_{3'2'}}{E^Y_{1'}E^Y_{2'}\Delta}; \quad C^Y_{1'3'} = \frac{\nu^Y_{2'3'} + \nu^Y_{2'1'}\nu^Y_{1'3'}}{E^Y_{1'}E^Y_{3'}\Delta}; \quad C^Y_{2'3'} = \frac{\nu^Y_{3'1'} + \nu^Y_{2'1'}\nu^Y_{3'2'}}{E^Y_{2'}E^Y_{3'}\Delta} \quad (27)$$

and

$$C^Y_{4'4'} = G^Y_{1'2'}; \quad C^Y_{5'5'} = G^Y_{2'3'}; \quad C^Y_{6'6'} = G^Y_{1'3'} \quad (28)$$

$$\Delta = \frac{1}{E^Y_{1'}E^Y_{2'}E^Y_{3'}} \begin{vmatrix} 1 & -\nu^Y_{2'1'} & -\nu^Y_{3'1'} \\ -\nu^Y_{1'2'} & 1 & -\nu^Y_{3'2'} \\ -\nu^Y_{1'3'} & -\nu^Y_{2'3'} & 1 \end{vmatrix} \quad (29)$$

Using the various C_{pq}, one can then calculate the parameters $A_1, A_2, \ldots A_9$ using the relations given in Andrianopoulos and Dernikas.[30] Dropping, for brevity, superscript Y, one may express them as

$$A_1 = \frac{1}{2D}\left[(C_{1'1'} + C_{1'2'} + C_{1'3'})^2 + C_{1'1'}(C_{2'2'} + 2C_{2'3'} + C_{3'3'}) - (C_{1'2'} + C_{1'3'})^2\right] \quad (30)$$

$$A_2 = \frac{1}{2D}\left[(C_{1'2'} + C_{2'2'} + C_{2'3'})^2 + C_{2'2'}(C_{1'1'} + 2C_{1'3'} + C_{3'3'}) - (C_{1'2'} + C_{2'3'})^2\right] \quad (31)$$

$$A_3 = \frac{1}{2D}\left[(C_{1'3'} + C_{2'3'} + C_{3'3'})^2 + C_{3'3'}(C_{1'1'} + 2C_{1'2'} + C_{2'2'}) - (C_{1'3'} + C_{2'3'})^2\right] \quad (32)$$

$$A_4 = \frac{1}{2D}[2(C_{1'1'} + C_{1'2'} + C_{1'3'})(C_{1'2'} + C_{2'2'} + C_{2'3'}) + \left(2C^2_{1'2'} - (C_{1'1'} + C_{1'3'})(C_{2'2'} + C_{2'3'}) + C_{1'2'}(C_{1'3'} + C_{2'3'} + C_{3'3'})\right)] \quad (33)$$

$$A_5 = \frac{1}{2D}[2(C_{1'2'} + C_{2'2'} + C_{2'3'})(C_{1'3'} + C_{2'3'} + C_{3'3'}) + 2(C_{2'3'}(C_{1'1'} + C_{2'3'}) + C_{1'3'}(-C_{2'2'} + C_{2'3'}) - C_{2'2'}C_{3'3'} - C_{1'2'}(C_{1'3'} - C_{2'3'} + C_{3'3'}))] \quad (34)$$

$$A_6 = \frac{1}{2D}[2(C_{1'3'} + C_{2'3'} + C_{3'3'})(C_{1'1'} + C_{1'2'} + C_{1'3'}) + 2(C_{1'3'}(C_{1'3'} + C_{2'2'} + C_{2'3'}) - C_{1'1'}(C_{2'3'} + C_{3'3'}) - C_{1'2'}(-C_{1'3'} + C_{2'3'} + C_{3'3'}))] \quad (35)$$

$$A_7 = C_{4'4'}/2 \quad A_8 = C_{5'5'}/2 \quad A_9 = C_{6'6'}/2 \quad (36)$$

where

$$D = C_{1'1'} + C_{2'2'} + C_{3'3'} + 2C_{1'2'} + 2C_{1'3'} + 2C_{2'3'} \quad (37)$$

Thus, using the computed values of $A_1, A_2, \ldots A_9$ and equations (16) to (19), one can obtain the stiffness tensor for one microplane. The foregoing expressions were derived by expressing the elastic strain energy density for anisotropic materials as the sum of the volumetric and deviatoric parts (for more details, see Andrianopoulos and Dernikas).[30]

Summary of calculation of the orthotropic stiffness constants

The proposed formulation computes the stiffness tensor of the RUC starting from the individual meso-scale constituents and then systematically proceeds to the macro-scale [Matrix + Fibers → Yarn → Microplane → Yarn plate → RUC]. This lends the model a hierarchical multi-scale character. To summarize, the procedure consists of five steps:

1. Obtain the effective properties of the yarn from the properties of the matrix and the fiber, given by equations (20) to (24);
2. Calculate the components of the elasticity tensor of the yarn, by considering it to be a unidirectional composite, given by equations (26) to (29);
3. Calculate the pre-multipliers $A_1, A_2, \ldots$, given by equations (30) to (37);
4. Calculate the stiffness tensor for the fill and warp yarn plates from the pre-multipliers and the microplane orientations;
5. Calculate the stiffness tensor of the RUC using equation (7).

Validation of the model for different weave architectures

The model is now used to compute the elastic properties of various woven composites. For any given weave type, the following inputs are required:

1. Elastic properties of the matrix;
2. Elastic properties of the fiber;
3. Volume fractions of the fiber within the yarn, V_f^Y, and within one RUC, V_f (which yields V_y);
4. Undulation angle α (which yields the microplane orientations);

Typically the properties of interest are the axial moduli, the shear modulus and the in-plane Poisson ratio of the composite. These are obtained by calculating the 6×6 compliance matrix of an RUC $[C^{RUC}] = [K^{RUC}]^{-1}$ and then using the following relations

$$E_1 = E_2 = \frac{1}{C^{RUC}(1,1)}; \quad \nu_{12} = -\frac{C^{RUC}(1,2)}{C^{RUC}(1,1)}; \quad G_{12} = \frac{1}{C^{RUC}(4,4)} \quad (38)$$

Plain woven composites

A plain weave consists of each fill yarn skipping over every other warp yarn. For this weave, the RUC is shown by the dashed square in Figure 4(a). The undulating yarn for a plain weave is discretized as shown in Figure 4(b). One microplane triad is introduced per segment, and equal weights are assigned to each microplane ($\omega^\mu = 1/6$ for all μ).

To evaluate the model, we choose a data set for plain woven composites from Ishikawa et al.[33] This composite consisted of T-300 carbon fibers and epoxy resin 3601. The properties of individual constituents, as listed in Ishikawa et al.[33] are shown in Table 1. The volume fraction of the fiber within one RUC was 0.58, while that within one yarn was about 0.65. Then, the volume fraction of the yarns (fill + warp) V_y within one RUC is given by equation (2) as 0.89 and then the volume fraction of the matrix outside the yarn is 0.11. The yarn properties shown in the table are calculated according to equations (20) to (24).

The ratio of the minor to major axis of the elliptical yarn cross section was 0.096. Assuming no gaps, the orientation of the inclined microplanes, $\alpha = 5.484$ deg. With these inputs, one computes the RUC stiffness tensor, and equation (38) then yields the required elastic constants. Their values are compared against the experimental values in Table 2. It is seen that the agreement is very good, for not only the axial moduli but also the in-plane Poisson ratio and the shear modulus.

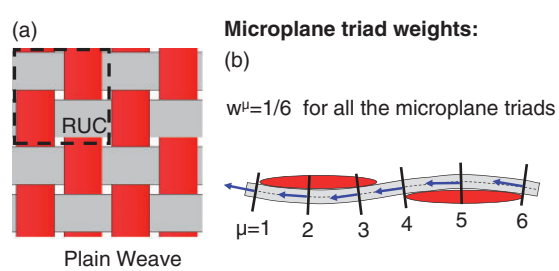

Figure 4. Schematic representation of (a) an RUC for a plain weave composite; (b) the microplane triads used for the discretization of the yarns.
RUC: representative unit cell.

To get the off-axis properties, the stiffness matrix is first rotated about axis 3 of the RUC. The compliance matrix is calculated, and equations (20) to (24) then yield the corresponding elastic constants. Three orientations are considered, viz. (1) 15/−75, (2) 30/−60, and (3) 45/−45. The predicted elastic constants are compared to experimental values in Table 3. While the off-axis properties are slightly underestimated, the overall agreement is very good. These underestimations are consistent with the CLT. To explain it, consider the 45° case. According to the CLT

$$\frac{1}{E_x} = \frac{c^4}{E_1} + \frac{s^4}{E_2} + s^2c^2\left(\frac{1}{G_{12}} - \frac{\nu_{12}}{E_1}\right) \tag{39}$$

Table 1. Mechanical properties of the constituents for epoxy 3601/carbon T-300 plain woven composite.[33]

Elastic constant	Matrix	Fiber	Yarn
Axial modulus $E_{1'}$ [GPa]	4.511 ($=E^m$)	208.8	137.3
Transverse modulus $E_{2'} = E_{3'}$ [GPa]	4.511 ($=E^m$)	43	10.65
Shear modulus $G_{1'2'} = G_{1'3'}$ [GPa]	1.7 ($=G^m$)	7.42	5.38
Shear modulus $G_{2'3'}$ [GPa]	1.7 ($=G^m$)	7.42	3.8
Poisson ratio $\nu_{1'2'} = \nu_{1'3'}$	0.38 = (ν^m)	0.2	0.263
Poisson ratio $\nu_{2'3'}$	0.38 = (ν^m)	0.499	0.4574

Table 2. Comparison of measured and predicted elastic constants for an epoxy 3601/carbon T-300 plain woven composite lamina.[33]

Elastic constant	Configuration	Experiment	Prediction
$E_1 = E_2$ [GPa]	0/90	63.1	64.92
$\nu_{12} = \nu_{21}$	0/90	0.053	0.019
G_{12} [GPa]	0/90	5.56	4.188
$E_1 = E_2$ [GPa]	45/−45	19.5	14.87
$\nu_{12} = \nu_{21}$	45/−45	0.75	0.775
G_{12} [GPa]	45/−45	30	31.84

where E_x is the off-axis axial modulus, E_1, E_2, and G_{12} are the various on-axis moduli, and s and c are the sine and cosine of the angle. Since $E_1 = E_2 \gg G_{12}$, one may approximate the above as

$$\frac{1}{E_x} \approx \frac{s^2c^2}{G_{12}} \quad \text{or} \quad E_x \approx 4G_{12} \quad \text{at } 45^\circ \tag{40}$$

The above equation implies that an underestimation of G_{12} in the on-axis configuration translates to underestimation of E_1 in the off-axis configuration. Similarly, an overestimation of on-axis E_1 would translate to an overestimation of off-axis G_{12}. This helps clarify why the present model tends to underestimate the off-axis stiffness. Anyway, a big improvement over the earlier microplane model for braided composites is obtained.

Consider now the data from Scida et al.[10] on plain woven composites consisting of a vinylester matrix and E-glass fibers. For these data, the properties of the individual constituents are unavailable, but those of the yarn are. So, the known range of the resin and fiber properties is used. The exact values are adjusted until the desired yarn properties are obtained; (see Table 4). For this weave, the fiber volume fractions with respect to the yarn and the RUC are 0.800 and 0.549, respectively. Accordingly, the volume fraction of the yarn within one RUC is 0.687.

The ratio of the minor to major axis of the yarn cross section is 0.0833. This implies the orientation angle of $\alpha = 4.76^\circ$. With these parameters, the axial

Table 3. Comparison of measured and predicted on and off-axis elastic moduli of an epoxy 3601/carbon T-300 plain woven composite lamina.[33]

Elastic constant	Orientation	Experiment	Prediction
$E_1 = E_2$ [GPa]	0/90	63.1	64.92
$E_1 = E_2$ [GPa]	15/−75	46.8	35.26
$E_1 = E_2$ [GPa]	30/−60	22	18.42
$E_1 = E_2$ [GPa]	45/−45	19.5	14.87

Table 4. Mechanical properties of the constituents for vinylester/E-glass plain woven composite.[10]

Elastic constant	Matrix	Fiber	Yarn	Yarn (target value from)[10]
Axial modulus $E_{1'}$ [GPa]	4.1 ($=E^m$)	71	57.62	57.5
Transverse modulus $E_{2'} = E_{3'}$ [GPa]	3.5 ($=E^m$)	71	16.65	18.8
Shear modulus $G_{1'2'} = G_{1'3'}$ [GPa]	1.485 ($=G^m$)	16.5	7.46	7.44
Shear modulus $G_{2'3'}$ [GPa]	1.485 ($=G^m$)	16.5	5.46	–
Poisson ratio $\nu_{1'2'} = \nu_{1'3'}$	0.38 = (ν^m)	0.22	0.252	0.25
Poisson ratio $\nu_{2'3'}$	0.38 = (ν^m)	0.49	0.468	–

and shear moduli, and the in-plain Poisson ratio, are calculated from equations (20) to (24) and are compared with the experimental results in Table 5. As can be seen, the agreement is good, which serves as an additional validation of the model.

Twill woven composites

The model is now extended to different weave types. Consider a twill weave, for which the fill yarn skips over two warp yarns per weave (Figure 5(a) and (b)). The data are obtained from Scida et al.[10] where tests of E-glass/epoxy composites are reported. For these tests, the properties of individual constituents are again unavailable, but those of the yarn are. So, the resin and fiber properties are adjusted within their known range until the desired yarn properties are obtained (as shown in Table 6). The fiber volume fractions for this weave with respect to the yarn and the RUC are 0.75 and 0.383, respectively. Accordingly, the volume fraction of the yarn within one RUC is 0.5106. The ratio of the minor to major axis of the yarn cross section is 0.1084, which implies the microplane orientation angle of $\alpha = 6.18^\circ$. Based on these parameters, the axial and shear moduli, and the in-plain Poisson ratio, are calculated from equations (20) to (24).

Table 5. Comparison of measured and predicted elastic moduli of a E-glass/vinylester plain woven composite.[10]

Elastic constant	Experiment	Prediction
$E_1 = E_2$ [GPa]	24.8 ± 1.1	27.71
ν_{12}	0.12 ± 0.01	0.098
G_{12} [GPa]	6.5 ± 0.8	5.58

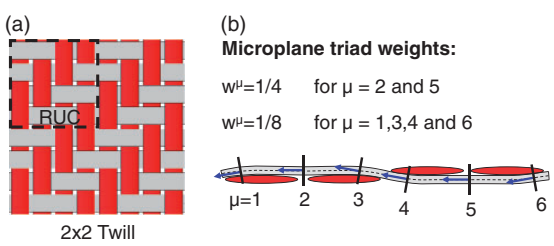

Figure 5. Schematic representation of (a) an RUC for a 2×2 twill weave composite; (b) the microplane triads used for the discretization of the yarns.
RUC: representative unit cell.

The weights of the microplane triads are decided based on dividing each ellipse into three parts, and then drawing the discretized undulation path. The path consists of six segments, each corresponding to one microplane triad. The weight assigned to the triad is proportional to the fraction of the yarn length occupied by that segment. So, for a twill weave, the weights are 1/8, 1/4, 1/8, 1/8, 1/4, and 1/8. Using the foregoing microplane orientations, weights, volume fractions, and the constituent properties, the stiffness tensor of the RUC K^{RUC} can be calculated. This yields the elastic properties of the laminate. Table 7 documents very good agreement between the measured and predicted values. Versatility and applicability to various weave patterns is thus demonstrated.

Harness satin woven composites

The 8-harness satin weave is a fabric in which the fill yarn alternately skips over one and then seven warp yarns and vice versa. The unit cell for this weave and the discretization of the undulating yarn are shown in Figure 6(a) and (b). Again, six segments along the yarn are used, implying six microplane triads, with different weights. Each yarn segment between two inflexion points is divided into three equal parts Figure 6(b), and then the weights of the six microplane triads are 1/24, 1/24, 1/24, 1/24, 19/24, 1/24. The higher weight is thus assigned to the non-inclined segment.

The data set for this weave is also available in[33] both for on- and off-axis properties. The constituent properties are the same as in Table 1. The fiber volume fractions for this weave, with respect to the yarn and the RUC, are 0.65 and 0.62, respectively. Accordingly, the volume fraction of the yarn within one RUC is 0.9692. The yarn cross section is more circular for this weave, and the ratio of minor to major axis is 0.35. So, the

Table 6. Mechanical properties of the constituents for epoxy/E-glass twill woven composite.[10]

Elastic constant	Matrix	Fiber	Yarn	Yarn (target value from)[10]
Axial modulus $E_{1'}$ [GPa]	4.1 ($=E^m$)	73	57.62	55.7
Transverse modulus $E_{2'} = E_{3'}$ [GPa]	4.1 ($=E^m$)	73	14.03	18.5
Shear modulus $G_{1'2'} = G_{1'3'}$ [GPa]	1.485 ($=G^m$)	14.5	6.14	6.15
Shear modulus $G_{2'3'}$ [GPa]	1.485 ($=G^m$)	14.5	4.545	–
Poisson ratio $\nu_{1'2'} = \nu_{1'3'}$	$0.38 = (\nu^m)$	0.167	0.2203	0.22
Poisson ratio $\nu_{2'3'}$	$0.38 = (\nu^m)$	0.49	0.4625	–

Table 7. Comparison of measured and predicted elastic moduli of a E-glass/epoxy twill woven composite.[10]

Elastic constant	Experiment	Prediction
$E_1 = E_2$ [GPa]	19.24 ± 0.13	20.42
ν_{12}	0.13 ± 0.004	0.107
G_{12} [GPa]	3.59 ± 0.03	3.86

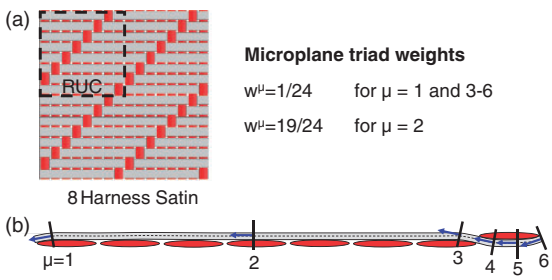

Figure 6. Schematic representation of (a) an RUC for a 8-harness satin composite; (b) the microplane triads used for the discretization of the yarns.
RUC: representative unit cell

Table 8. Comparison of measured and predicted elastic constants for an epoxy 3601/carbon T-300 8-harness satin woven composite.[33]

Elastic constant	Configuration	Experiment	Prediction
$E_1 = E_2$ [GPa]	0/90	65.2	68.35
$\nu_{12} = \nu_{21}$	0/90	0.061	0.012
G_{12} [GPa]	0/90	5.3	4.42
$E_1 = E_2$ [GPa]	45/−45	18	15.68
$\nu_{12} = \nu_{21}$	45/−45	0.7	0.773
G_{12} [GPa]	45/−45	30.7	33.78
$E_1 = E_2$ [GPa]	22.5/−67.5	34.7	25.5

undulation angle is higher in this case and is equal to 19.28°. Using these parameters, the elastic properties, both on and off-axis, were predicted. Their comparison against experimental data is shown in Table 8. It is seen that the agreement is again very good, though with slight underestimation of the off-axis properties.

Conclusions

1. Multi-scale adaptation of the microplane model to woven composites makes it possible to get rather accurate predictions of all the orthotropic elastic constants from the constituent properties and the weave architecture, including the plain, twill and satin weaves.
2. The new microplane model for woven composites captures the lower-scale effects of yarn undulations and of the cross section aspect ratio on the orthotropic elastic constants of the composite. The feature that makes this possible is that the constituent elastic properties are characterized in the microplane model in a vectorial form, which allows simple, clear, and physically sound conceptual interpretation of the mechanical behavior on the meso-scale.
3. The macro-scale constitutive behavior is derived from the meso-scale model of the fibers, yarn, and polymer matrix. It is this multi-scale feature that leads to high-fidelity predictions.
4. The possibility to predict the orthotropic elastic constants from the constituent properties reduces the need for repeat testing of similar composites with small differences in composition or weave type, or both.
5. The formulation has sufficient generality to allow extensions to composites with more complex architectures, such as the hybrid woven composites, and two- or three-dimensionally braided composites.
6. Compared to the previous microplane model for the orthotropic elastic constants of the triaxially braided composite,[27] the improvements consist of significantly better predictions of the shear stiffness and Poisson effects (especially for off-axis cases). This is achieved by: (a) deriving the microplane stiffness tensor from all the components of strain energy, and (b) representing the yarn segments of different inclinations by triads of orthogonal microplanes in which the transverse interactions can be captured in a simple way.
7. Although the off-axis predictions are slightly less accurate than the 3D finite element modeling of the elastic constants of the RUC, they are still perfectly acceptable for practical purposes. Thus, the model achieves proper balance between accuracy of prediction and computational efficiency, which is what the detailed finite element models of the RUC lack.
8. The present model is readily extendable to microplane finite element analysis of large composite structures in which material damage alters the elastic moduli matrix of each RUC. By contrast, the 3D finite element analysis of the orthotropic constants would be computationally prohibitive, since it would have to be run for each finite element in each time step. This is where the main advantage of the present model lies.

Declaration of Conflicting Interests

The author(s) declared no potential conflicts of interest with respect to the research, authorship, and/or publication of this article.

Funding

The author(s) disclosed receipt of the following financial support for the research, authorship, and/or publication of this article: Partial support has been obtained under US National Science Foundation Grant CMMI-1439950 and under Office of Naval Research Grant NOOO14-11-1-0515, both to Northwestern University. Some applications are currently being studied under Grant SP0020579 to Northwestern University from US Department of Energy through the US Council for Automotive Research.

References

1. Tan P, Tong L and Steven GP. Modelling for predicting the mechanical properties of textile composites – a review. *Compos Part A* 1997; 28: 903–922.
2. Hallal A, Younes R and Fardoun F. Review and comparative study of analytical modeling for the elastic properties of textile composites. *Compos Part B* 2013; 50: 22–31.
3. Dixit A and Mali HS. Modeling techniques for predicting the mechanical properties of woven-fabric textile composites: a review. *Mech Comp Mater* 2013; 49: 3–30.
4. Bažant ZP. Effect of folding of reinforcing fibers on the elastic moduli and strength of composite materials (in Russian). *Mekhanika Polimerov (Riga)* 1968; 4: 314–321. (journal available in English translation as Mechanics of Polymers).
5. Bažant ZP and Cedolin L. *Stability of structures: elastic, inelastic, fracture and damage theories*. New York: Oxford University Press, 1991. (2nd ed. Dover Publ.; 3rd ed. World Scientific Publishing: Singapore/New Jersey/London, 2010).
6. Ishikawa T and Chou TW. Stiffness and strength behavior of woven fabric composites. *J Mater Sci* 1982; 17: 3211–3220.
7. Ishikawa T and Chou TW. One-dimensional micromechanical analysis of woven fabric composites. *AIAA J* 1983; 21: 1714–1421.
8. Naik NK and Ganesh VK. Prediction of on-axes elastic properties of plain weave fabric composites. *Compos Sci Tech* 1992; 45: 135–152.
9. Hahn HT and Pandey R. A micromechanics model for thermoelastic properties of plain weave fabric composites. *J Eng Mater Tech* 1994; 116: 517–523.
10. Scida D, Aboura Z, Benzeggagh ML, et al. Prediction of the elastic behavior of hybrid and non-hybrid woven composites. *Compos Sci Tech* 1997; 57: 1727–1740.
11. Zhang YC and Harding J. A numerical micromechanics analysis of the mechanical properties of a plain weave composite. *Comput Struct* 1990; 36: 839–849.
12. Blackketter DM, Walrath DE and Hansen AC. Modeling damage in a plain weave fabric-reinforced composite material. *J Compos Tech Res* 1993; 15: 136–142.
13. Carvelli V and Poggi C. A homogenization procedure for the numerical analysis of woven fabric composites. *Compos Part A* 2001; 32: 1425–1432.
14. Lomov SV, Huysmans G, Luo Y, et al. Textile composites: modelling strategies. *Compos Part A* 2001; 32: 1379–1394.
15. Chapalkar P and Kelkar AD. Classical laminate theory model for twill weave fabric. *Compos Part A* 2001; 32: 1281–1289.
16. Quek SC, Waas AM, Shahwan KW, et al. Analysis of 2D triaxial flat braided textile composites. *Int J Mech Sci* 2003; 45: 1077–1096.
17. Sankar BV and Marrey RV. A unit-cell model of textile composite beams for predicting stiffness properties. *Compos Sci Tech* 1993; 49: 61–69.
18. Cox BN, Carter WC and Fleck NA. A binary model of textile composites-I, formulation. *Actu Metallurgical et Materiulia* 1994; 42: 3463–3479.
19. Bažant ZP and Oh BH. Microplane model for progressive fracture of concrete and rock. *J Eng Mech ASCE* 1985; 111: 559–582.
20. Bažant ZP, Caner FC, Carol I, et al. Microplane model M4 for concrete. I: formulation with work-conjugate deviatoric stress. *J Eng Mech ASCE* 2000; 126: 944–953.
21. Caner FC and Bažant ZP. Microplane model M7 for plain concrete. I: formulation. *J Eng Mech ASCE* 2013; 139: 1714–1723.
22. Taylor GI. Plastic strain in metals. *J Inst Metals* 1938; 62: 307–324.
23. Brocca M and Bažant ZP. Microplane constitutive model and metal plasticity. *Appl Mech Rev ASME* 2000; 53: 265–281.
24. Brocca M, Bažant ZP and Daniel IM. Microplane model for stiff foams and finite element analysis of sandwich failure by core indentation. *Int J Solids Struct* 2001; 38: 8111–8132.
25. Cusatis G, Beghini A and Bažant ZP. Spectral stiffness microplane model for quasibrittle composite laminates-Part I: Theory. *J Appl Mech* 2008; 75: 0210091–8.
26. Beghini A, Cusatis G and Bažant ZP. Spectral stiffness microplane model for quasibrittle composite laminates – Part II: calibration and validation. *J Appl Mech* 2008; 75: 0210101–6.
27. Caner FC, Bažant ZP, Hoover CG, et al. Microplane Model for fracturing damage of triaxially braided fiber-polymer composites. *J Appl Mech* 2011; 133: 0210241–12.
28. Chou TW. *Microstructural design of fibre composites*. New York: Cambridge University Press, 1992.
29. Bogdanovich AE and Pastore CM. *Mechanics of textile and laminated composites*. London: Chapman and Hall, 1996.
30. Andrianopoulos NP and Dernikas IT. An attempt to separate elastic strain energy density of linear elastic anisotropic materials based on strains considerations. *Acta Mech* 2013; 224: 1879–1885.
31. Hashin Z and Rosen B. "The elastic moduli of fiber-reinforced materials". *J Comp Mat* 1964; 31: 223–232.
32. Daniel IM and Ishai O. *Engineering mechanics of composite materials*. New York: Oxford University Press, 1992.
33. Ishikawa T, Matsushima M, Hayashi Y, et al. Experimental confirmation of the theory of elastic moduli of fabric composites. *J Comp Mat* 1985; 19: 443–458.

Appendix

For additional clarity, we demonstrate the construction of the complete stiffness tensor for one microplane triad for which $\mathbf{n}=[1,\ 0,\ 0]$, $\mathbf{m}=[0,\ 1,\ 0]$ and $\mathbf{l}=[0,\ 0,\ 1]$. For the sake of convenience we introduce Kelvin notation. So, $n_i n_j n_k n_l = N_I N_J$, $m_i m_j m_k m_l = M_I M_J$ and $l_i l_j l_k l_l = L_I L_J$ where I and $J=1$ to 6. Then

$$N_I N_J = \begin{bmatrix} 1 & 0 & 0 & 0 & 0 & 0 \\ 0 & 0 & 0 & 0 & 0 & 0 \\ 0 & 0 & 0 & 0 & 0 & 0 \\ 0 & 0 & 0 & 0 & 0 & 0 \\ 0 & 0 & 0 & 0 & 0 & 0 \\ 0 & 0 & 0 & 0 & 0 & 0 \end{bmatrix}$$

$$M_I M_J = \begin{bmatrix} 0 & 0 & 0 & 0 & 0 & 0 \\ 0 & 1 & 0 & 0 & 0 & 0 \\ 0 & 0 & 0 & 0 & 0 & 0 \\ 0 & 0 & 0 & 0 & 0 & 0 \\ 0 & 0 & 0 & 0 & 0 & 0 \\ 0 & 0 & 0 & 0 & 0 & 0 \end{bmatrix} \tag{41}$$

$$L_I L_J = \begin{bmatrix} 0 & 0 & 0 & 0 & 0 & 0 \\ 0 & 0 & 0 & 0 & 0 & 0 \\ 0 & 0 & 1 & 0 & 0 & 0 \\ 0 & 0 & 0 & 0 & 0 & 0 \\ 0 & 0 & 0 & 0 & 0 & 0 \\ 0 & 0 & 0 & 0 & 0 & 0 \end{bmatrix}$$

Thus

$$K_{IJ}^{N\mu} = \begin{bmatrix} 2A_1 & 0 & 0 & 0 & 0 & 0 \\ 0 & 2A_2 & 0 & 0 & 0 & 0 \\ 0 & 0 & 2A_3 & 0 & 0 & 0 \\ 0 & 0 & 0 & 0 & 0 & 0 \\ 0 & 0 & 0 & 0 & 0 & 0 \\ 0 & 0 & 0 & 0 & 0 & 0 \end{bmatrix} \tag{42}$$

Furthermore, $n_i n_j m_k m_l = N_I M_J$, $n_i n_j l_k l_l = N_I L_J$ and $m_i m_j l_k l_l = M_I L_J$. Then

$$N_I M_J = \begin{bmatrix} 0 & 1 & 0 & 0 & 0 & 0 \\ 0 & 0 & 0 & 0 & 0 & 0 \\ 0 & 0 & 0 & 0 & 0 & 0 \\ 0 & 0 & 0 & 0 & 0 & 0 \\ 0 & 0 & 0 & 0 & 0 & 0 \\ 0 & 0 & 0 & 0 & 0 & 0 \end{bmatrix}$$

$$M_I N_J = \begin{bmatrix} 0 & 0 & 0 & 0 & 0 & 0 \\ 1 & 0 & 0 & 0 & 0 & 0 \\ 0 & 0 & 0 & 0 & 0 & 0 \\ 0 & 0 & 0 & 0 & 0 & 0 \\ 0 & 0 & 0 & 0 & 0 & 0 \\ 0 & 0 & 0 & 0 & 0 & 0 \end{bmatrix} \tag{43}$$

$$N_I L_J = \begin{bmatrix} 0 & 0 & 1 & 0 & 0 & 0 \\ 0 & 0 & 0 & 0 & 0 & 0 \\ 0 & 0 & 0 & 0 & 0 & 0 \\ 0 & 0 & 0 & 0 & 0 & 0 \\ 0 & 0 & 0 & 0 & 0 & 0 \\ 0 & 0 & 0 & 0 & 0 & 0 \end{bmatrix}$$

$$L_I N_J = \begin{bmatrix} 0 & 0 & 0 & 0 & 0 & 0 \\ 0 & 0 & 0 & 0 & 0 & 0 \\ 1 & 0 & 0 & 0 & 0 & 0 \\ 0 & 0 & 0 & 0 & 0 & 0 \\ 0 & 0 & 0 & 0 & 0 & 0 \\ 0 & 0 & 0 & 0 & 0 & 0 \end{bmatrix} \tag{44}$$

$$M_I L_J = \begin{bmatrix} 0 & 0 & 0 & 0 & 0 & 0 \\ 0 & 0 & 1 & 0 & 0 & 0 \\ 0 & 0 & 0 & 0 & 0 & 0 \\ 0 & 0 & 0 & 0 & 0 & 0 \\ 0 & 0 & 0 & 0 & 0 & 0 \\ 0 & 0 & 0 & 0 & 0 & 0 \end{bmatrix}$$

$$L_I M_J = \begin{bmatrix} 0 & 0 & 0 & 0 & 0 & 0 \\ 0 & 0 & 0 & 0 & 0 & 0 \\ 0 & 1 & 0 & 0 & 0 & 0 \\ 0 & 0 & 0 & 0 & 0 & 0 \\ 0 & 0 & 0 & 0 & 0 & 0 \\ 0 & 0 & 0 & 0 & 0 & 0 \end{bmatrix} \tag{45}$$

Thus

$$K_{IJ}^{P\mu} = \begin{bmatrix} 0 & A_4/2 & A_5/2 & 0 & 0 & 0 \\ A_4/2 & 0 & A_6/2 & 0 & 0 & 0 \\ A_5/2 & A_6/2 & 0 & 0 & 0 & 0 \\ 0 & 0 & 0 & 0 & 0 & 0 \\ 0 & 0 & 0 & 0 & 0 & 0 \\ 0 & 0 & 0 & 0 & 0 & 0 \end{bmatrix} \tag{46}$$

and

$$A_I A_J = \begin{bmatrix} 0 & 0 & 0 & 0 & 0 & 0 \\ 0 & 0 & 0 & 0 & 0 & 0 \\ 0 & 0 & 0 & 0 & 0 & 0 \\ 0 & 0 & 0 & 1 & 0 & 0 \\ 0 & 0 & 0 & 0 & 0 & 0 \\ 0 & 0 & 0 & 0 & 0 & 0 \end{bmatrix}$$

$$B_I B_J = \begin{bmatrix} 0 & 0 & 0 & 0 & 0 & 0 \\ 0 & 0 & 0 & 0 & 0 & 0 \\ 0 & 0 & 0 & 0 & 0 & 0 \\ 0 & 0 & 0 & 0 & 0 & 0 \\ 0 & 0 & 0 & 0 & 1 & 0 \\ 0 & 0 & 0 & 0 & 0 & 0 \end{bmatrix} \tag{47}$$

$$C_I C_J = \begin{bmatrix} 0 & 0 & 0 & 0 & 0 & 0 \\ 0 & 0 & 0 & 0 & 0 & 0 \\ 0 & 0 & 0 & 0 & 0 & 0 \\ 0 & 0 & 0 & 0 & 0 & 0 \\ 0 & 0 & 0 & 0 & 0 & 0 \\ 0 & 0 & 0 & 0 & 0 & 1 \end{bmatrix}$$

Thus

$$K_{IJ}^{S\mu} = \begin{bmatrix} 0 & 0 & 0 & 0 & 0 & 0 \\ 0 & 0 & 0 & 0 & 0 & 0 \\ 0 & 0 & 0 & 0 & 0 & 0 \\ 0 & 0 & 0 & 2A_7 & 0 & 0 \\ 0 & 0 & 0 & 0 & 2A_8 & 0 \\ 0 & 0 & 0 & 0 & 0 & 2A_9 \end{bmatrix} \tag{48}$$

Then the fully populated microplane triad stiffness tensor becomes

$$K_{IJ}^{\mu} = \begin{bmatrix} 2A_1 & A_4/2 & A_5/2 & 0 & 0 & 0 \\ A_4/2 & 2A_2 & A_6/2 & 0 & 0 & 0 \\ A_5/2 & A_6/2 & 2A_3 & 0 & 0 & 0 \\ 0 & 0 & 0 & 2A_7 & 0 & 0 \\ 0 & 0 & 0 & 0 & 2A_8 & 0 \\ 0 & 0 & 0 & 0 & 0 & 2A_9 \end{bmatrix} \tag{49}$$

It is thus demonstrated that, to calculate the complete stiffness tensor of a microplane triad in a rigorous manner, all the six strain vectors need to be considered.